Brief Communications

Death Receptor 6 Regulates Adult Experience-Dependent Cortical Plasticity

Sally A. Marik,[1] Olav Olsen,[2] Marc Tessier-Lavigne,[2] and Charles D. Gilbert[1]

[1]Laboratory of Neurobiology and [2]Laboratory of Brain Development and Repair, Rockefeller University, New York, New York 10065

Sensory experience alters cortical circuitry by parallel processes of axon outgrowth and pruning, but the mechanisms that control these rearrangements are poorly understood. Using *in vivo* 2-photon longitudinal imaging, we found a marked reduction in axonal pruning in somatosensory cortex of mice with a knock-out of the *DR6* gene, which codes for Death Receptor 6. This effect was seen for both long-range horizontal excitatory connections and for the axons of inhibitory neurons. These results identify a new pathway governing axonal plasticity associated with experience-dependent changes in cortical maps.

Introduction

Alterations in sensory experience lead to changes in cortical topographic sensory maps. A valuable model for studying the circuit mechanisms of experience-dependent cortical plasticity is the creation of a cortical lesion projection zone (LPZ) by selective elimination of peripheral sensory input to a restricted portion of the cortex, resulting in a sensory "blind" spot in the cortex (Fox, 1992). The altered sensory input impacts axonal morphology of layer 2/3 cortical pyramidal cells located within the cortical regions adjacent to the LPZ (peri-LPZ). Excitatory neurons outside the LPZ undergo simultaneous axonal sprouting and extensive pruning of existing axons that extend into the LPZ (Darian-Smith and Gilbert, 1994; Kossut and Juliano, 1999; Yamahachi et al., 2009; Marik et al., 2010), and the rate of dendritic spine turnover increases threefold within the LPZ (Keck et al., 2008). In addition, the axons of layer 2/3 inhibitory neurons within the LPZ also show massive outgrowth and parallel pruning (Marik et al., 2010). Such extensive changes in axonal arbors have been documented in macaque visual cortex after retinal lesions as well as in the mouse somatosensory cortex after whisker plucking. Changes in axonal arbors enable cortical neurons within the LPZ to recover sensory input, which is derived from neighboring regions of the cortical map, resulting in a shrinkage in the cortical representation of the lesioned part of the sensory surface and an expansion in the representation of the intact regions. In the visual system, this reorganization has adaptive value, mediating perceptual fill-in across retinal lesions (McManus et al., 2008). The rates of axonal growth and retraction are comparable with those seen for developing neurons in early postnatal mice (Portera-Cailliau et al., 2005) and are so rapid that they can be observed when axonal arbors are imaged hourly (Marik et al., 2010). Here, we focus on the mouse somatosensory model, as it is amenable to exploring the molecular mechanisms of cortical plasticity induced by altered sensory experience.

In the current study, we sought to investigate the molecular mechanisms leading from alterations in neuronal activity to the restructuring of axonal arbors. Prior data have suggested an involvement of the neurotrophin BDNF in triggering the axonal growth (Obata et al., 1999), but the mechanisms that control the adult pruning are unknown. A pathway of particular interest that has been revealed by *in vitro* and *in vivo* experiments is the death receptor 6 (DR6) pathway, which mediates axonal pruning in nervous system during development (Nikolaev et al., 2009). DR6 regulates axonal pruning after removal of trophic factors *in vitro* and in developmental pruning *in vivo* (Nikolaev et al., 2009), via a caspase-dependent pathway (Nikolaev et al., 2009; Simon et al., 2012). Here, we provide evidence that DR6 is also a key player in axonal retraction that accompanies experience-dependent plasticity in the adult.

Materials and Methods

Adult DR6 knock-out mice (Genentech) (Zhao et al., 2001) and wild-type (WT) littermates were used. Injections were done after P60, and the first imaging session was performed 3 weeks later. Data from WT mice from previously published work were pooled with WT data (Marik et al., 2010) because there was no significant difference between axonal pruning between the two populations of mice (t test, $p = 0.22$). No data were excluded from analysis. All procedures were performed in accordance with institutional and federal guidelines for the treatment of animals.

Virus preparation. Virus preparation was done as previously described (Marik et al., 2010). Briefly, two adeno-associated viruses (AAVs) were genetically engineered to label either excitatory or inhibitory neurons. Excitatory neurons were labeled with an AAV2 vector that contained the α-CaMKII promoter sequence and td-Tomato fluorescent protein sequence. Inhibitory neurons were labeled with an AAV2 vector that contained a truncated 2.7 kb promoter region of the *GAD65* gene and *eGFP* sequence. AAVs were packaged and purified according to previous published methods (Marik et al., 2010). Cell-type specificity was previously established by immunohistochemistry against calbindin, calretinin, and parvalbumin that collectively label 90% of all inhibitory neurons. Titer

Received June 6, 2013; revised July 18, 2013; accepted Aug. 9, 2013.

Author contributions: S.A.M. and C.D.G. designed research; S.A.M. and C.D.G. performed research; S.A.M., O.O., and C.D.G. analyzed data; S.A.M., O.O., M.T.-L., and C.D.G. wrote the paper.

This work was supported by National Institutes of Health Grant EY018119.

The authors declare no competing financial interests.

Correspondence should be addressed to Dr. Charles D. Gilbert, Laboratory of Neurobiology, Rockefeller University, 1230 York Avenue, New York, NY 10065. E-mail: gilbert@rockefeller.edu.

DOI:10.1523/JNEUROSCI.2398-13.2013

 0270-6474/13/3314998-06$15.00/0

was confirmed by RT-PCR and proper packaging of the AAV was confirmed by EM.

Surgery. A craniotomy, with dura intact, was performed over barrel cortex in adult male mice ($N = 21$) anesthetized with ketamine (80 mg/kg) and xylazine (6 mg/kg). The cortical topography of the barrel cortex was mapped electrophysiologically. One of the two high-titer preparations of AAV was injected into the cortex using nanoject glass capillaries and Nanoject II auto-nanoliter injector (Drummond) at a depth of 250–350 μm from the cortical surface. The dura was left intact throughout the procedure. The injections consisted of 40 nl αCaMKII.tdTomato.AAV (1×10^{12} particles/ml) placed in the C3 barrel column or 40 nl of GAD65.eGFP.AAV (2×10^{13} particles/ml) placed into either the deprived columns. A 3 mm circular glass coverslip was placed over the craniotomy and sealed with dental acrylic (Lang Dental Manufacturing), allowing imaging of neurons and their processes (Marik et al., 2010).

Imaging. Imaging began at least 3 weeks after the viral injection to ensure full expression of the virus. During imaging, animals were anesthetized with isoflurane (3% induction; 1.5–2% maintenance).

Images were collected on a custom-built 2-photon microscope that was modified from a Leica TCS Sp2 confocal microscope with a scanning head, which was moveable in three dimensions using a Sutter MP-285-3Z micromanipulator. The laser source was a Ti-sapphire laser (Tsunami/Millenia System, Spectra Physics). Images were acquired with Leica Confocal Software.

Whisker plucking. After the baseline imaging session(s), whiskers from rows D and E were plucked every other day to prevent new whisker growth and thereby to maintain deprivation of the D and E whisker barrel columns. Imaging was done for variable intervals after the onset of the deprivation period.

Analysis. Offline images were viewed with ImageJ (http://rsbweb.nih.gov/ij/) and deconvolved using Huygens deconvolution software (Scientific Volume Imaging). Axons were traced via the semiautomatic mode in Neuromantic (version 1.6.3; http://www.rdg.ac.uk/neuromantic/), and reconstruction's voxel size was corrected with a custom MATLAB (MathWorks) program.

We reconstructed a total of 1.45 m of labeled axonal arbors for this study. Tracings were done while viewing the axons and moving up and down through the *z*-stacks. After reconstruction, axons were coded as stable, pruned, or added in relation to baseline (see Figs. 2*a* and 3*a*) or in relation to the previous imaging session (see Fig. 2*b*). Axonal pruning and axonal growth were calculated by taking the axonal length of the class of axon (stable, prune, or added) for a given time point and dividing it by either the total length of axons present at baseline (see Figs. 2*a* and 3*a*) or from the previous time point (see Fig. 2*b*) and then reported as a percentage change. An axonal arbor was determined to possess an abnormal reversal if the axonal branch at one point deviated >90 degrees from the axis of projection of the axon.

Quantification of bouton dynamics was done for each axon by comparing images of the axon at different time points and noting all the boutons to determine those that were added, stable, or retracted. Quantification was done by two independent observers who were blinded to genotype, with identical results.

Axonal area was determined by tracing the outer edge of the axons reconstructed in manual mode of Neuromantic, which produces an SWC file, and calculated by a MATLAB (MathWorks) program that measures the area circumscribed by the points in the SWC file.

Statistical analysis. ANOVA was used to determine whether there was a statistical significance of axonal pruning between WT and *DR6* mutant animals across time points. Student's *t* test was used to determine statistical significance between genotypes at the same time point. *F* test was used to determine whether there was a statistical significance of initial area measurements between $DR6^{-/-}$ and WT. ANOVA was used to determine whether there was a statistical significance of bouton turnover across time points and genotypes. Student's *t* test was used to determine statistical significance of bouton turnover between genotypes at the same time point.

Results

We determined whether DR6 was required for axonal pruning in adult plasticity by imaging axonal structure before and after whisker plucking in functionally identified areas of the whisker barrel cortex of $DR6^{-/-}$ mice. This part of the mouse somatosensory cortex contains a representation of the facial whiskers as a series of rows of "barrels," with each barrel receiving primary input from one whisker. After plucking two rows of whiskers, the cortical representation of the adjacent row expanded into the deprived rows (or LPZ).

Using this approach, a previous study (Marik et al., 2010) showed that axonal arbors are static and fail to show gross morphological rearrangements in the absence of manipulation of sensory experience. However, when one functionally deafferents a portion of the sensory map, excitatory neurons lying outside the LPZ undergo massive sprouting into the LPZ. The sprouting is accompanied by pruning of portions of the preexisting axonal arbors, with a continuing turnover of the collaterals of excitatory layer 2/3 axons that starts immediately after whisker plucking and continues over a period of weeks. These changes are quite rapid. Just one day after whisker plucking, 77% of the original axonal arbors imaged were pruned.

Consistent with prior results (Marik et al., 2010), WT animals did not show any changes in excitatory axon arbors before plucking (data not shown) but experienced massive growth and pruning of excitatory axons after whisker plucking (based on a total of 650 mm of reconstructed axons in 16 animals; Fig. 1, left). Axons projecting into the LPZ were reconstructed and classified as stable, newly added, or retracted depending on their appearance over two imaging time points. The extent of axonal addition or subtraction was expressed as a percentage change relative to the length of axon present at baseline, before the start of plucking (Fig. 2*a*; dashed yellow lines indicate percentage added; dashed red lines indicate percentage subtracted). Because we were able to track identified axons longitudinally over multiple time points, we were also able to measure the effect of sensory manipulation over time. Here, we expressed the rate of change at each time point as a percentage of addition or subtraction in axonal length relative to the previous time point (Fig. 2*b*). The *in vivo* 2-photon imaging technique enabled us to show, as demonstrated previously, that whisker plucking was associated with parallel processes of sprouting and pruning of excitatory axons that continued for the full period over which we imaged, and that led to a net increase in the density of horizontally projecting axons in the LPZ.

Like WT animals, $DR6^{-/-}$ mice did not show any changes in excitatory axon arbors before sensory deprivation (Fig. 1); but in contrast to WT animals, they exhibited little to no pruning of horizontally projecting excitatory axons, based on a total of 419 mm of reconstructed axons in 14 $DR6^{-/-}$ animals (Fig. 2). Indeed, there was almost a complete lack of pruning of axonal arbors in $DR6^{-/-}$ mice (Figs. 1, right, and 2*a*,*b*) compared with WT (Figs. 1 left, and 2*a*,*b*). The difference in the amount of axonal pruning between WT and $DR6^{-/-}$ animals was highly significant ($p < 0.001$). Additionally, 2 d after whisker plucking, the percentage of new excitatory axons was significantly greater in *DR6* mutants than in WT animals (Fig. 2*a*). Because, in WT animals, newly formed axons are more subject to pruning than the original axons imaged at baseline (Yamahachi et al., 2009; Marik et al., 2010), we compared the amount of pruning of this axonal population in $DR6^{-/-}$ and WT littermates. Here, we calculated the percentage loss between successive imaging sessions

(Fig. 2*b*) and found that even the newly formed axons remained stable in the *DR6*$^{-/-}$ mice relative to WT (ANOVA, $p < 0.001$).

Another difference between *DR6*$^{-/-}$ and WT animals was the baseline extent of horizontally projecting axons in layer II/III before sensory deprivation, which was substantially greater in *DR6*$^{-/-}$ mice than in WT mice, suggesting a possible deficit in axonal pruning occurring during development (Fig. 1). The difference in axonal length between the two groups is reflected in the area that excitatory axons occupy during baseline imaging sessions. Excitatory axons initially occupied an area of 0.22 ± 0.05 mm^2 for *DR6*$^{-/-}$ mice, whereas axons of WT mice occupied an area 0.06 ± 0.04 mm^2 ($p = 0.03$, *F* test). Interestingly, axons of *DR6*$^{-/-}$ mice also showed abnormal trajectories, including awkward reversals (as defined in Materials and Methods) occurring at a rate of once every 0.95 mm of axon length (Fig. 2*c*). In contrast, among WT littermates where axonal pruning was common, newly extended axons lacked such awkward turns. If pruning is a mechanism to remove inappropriate projections, then abnormal trajectories in the knock-out might reflect a compensatory mechanism to correct inappropriate projections in these pruning-deficient animals or may reflect a contribution of DR6 signaling in axon guidance.

We next compared, in *DR6* and WT animals, changes in the axonal arbors of inhibitory interneurons located within the LPZ. Inhibitory interneurons were selectively labeled using a genetically engineered AAV that drove eGFP expression under control of a portion of the *GAD 65* promoter (Fig. 3*a*). WT inhibitory interneurons located within the LPZ underwent exuberant axonal growth into nondeprived cortex along with extensive pruning as previously reported (Marik et al., 2010). We imaged the neurons at day zero and then again 2 and 30 d after whisker plucking. Our analysis is based on a total of 247 mm of reconstructed axons in 4 WT animals and 137 mm of reconstructed axons in 6 *DR6*$^{-/-}$ animals (for an example of labeled axons, see Fig. 3*b*). For the *DR6*$^{-/-}$ mice, even before any whisker manipulation, the baseline extent of the axonal arbors of the labeled inhibitory neurons was substantially greater than those of the WT animals. Inhibitory axons at baseline occupied an area of 0.281 ± 0.105 mm^2 for *DR6*$^{-/-}$ mice, whereas those of WT mice occupied an area of 0.129 ± 0.004 mm^2 ($p = 0.02$, *F*

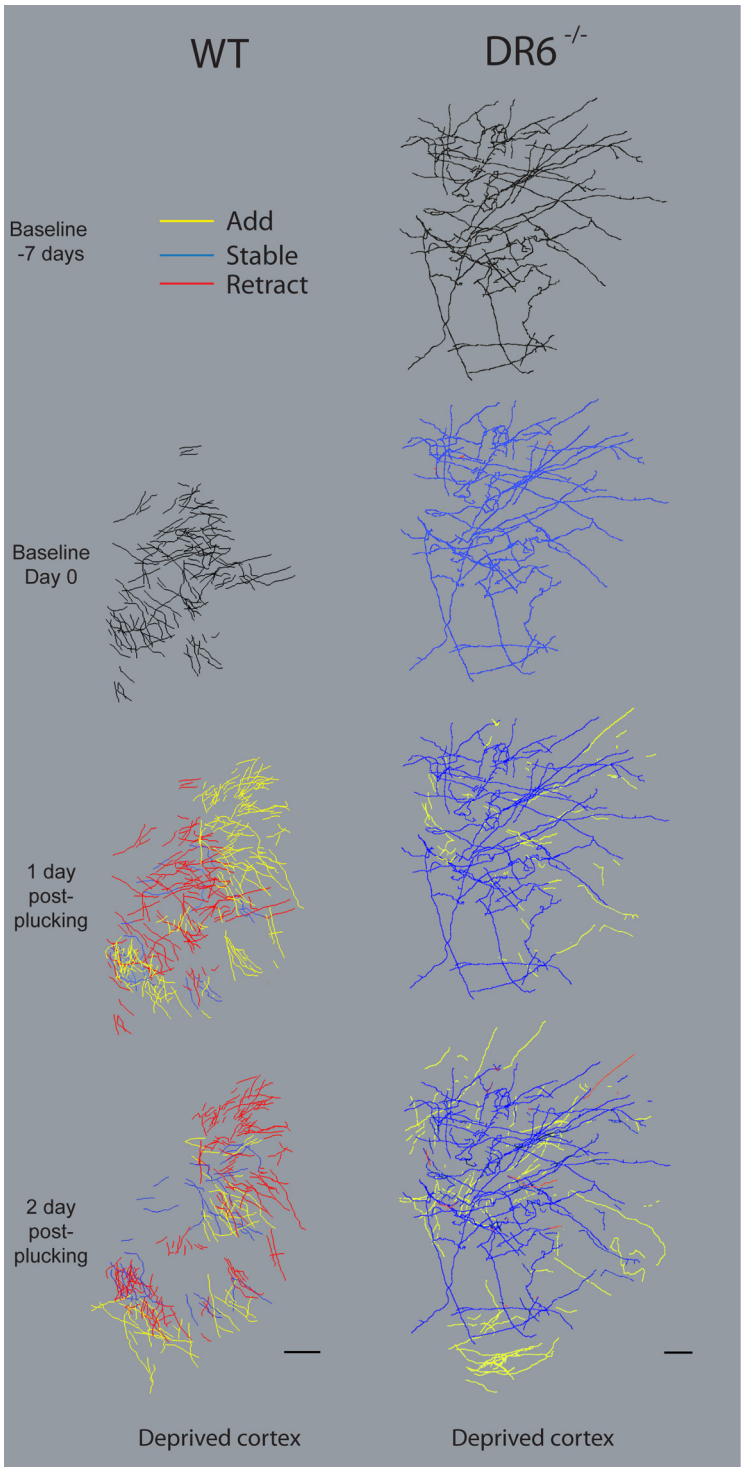

Figure 1. DR6 regulates axonal pruning of excitatory neurons associated with experience-dependent plasticity. Reconstructions of axonal arbors extending over rows D and E from two exemplar mice: one *DR6*$^{-/-}$ (right column) one WT (left column). Excitatory neurons located in C3 of WT littermates and *DR6*$^{-/-}$ mice were labeled with αCaMKII.tdTomato.AAV. Shown are reconstructed axons projecting into D and E rows over multiple days after plucking for both WT (left column) and *DR6*$^{-/-}$ mice (right column). Baseline control imaging sessions for *DR6*$^{-/-}$ were separated by 1 week ($N = 7$). Axons are color coded to represent one of four categories, as follows. Black represents initial image to which images from later time points are compared. Then, for each subsequent time point: blue represents axons that are stable compared with the time point immediately before the present one; red represents axons present at the time point immediately before this one that have been retracted at this time point; yellow represents axons that were newly added at this time point compared with the one immediately prior. Scale bar, 100 μm.

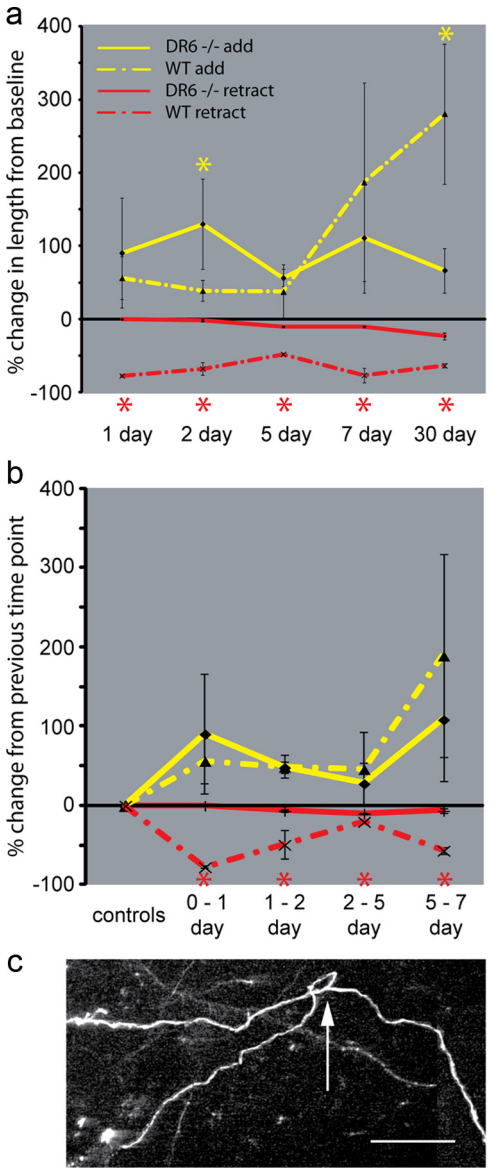

Figure 2. Quantification of axonal remodeling before and after whisker plucking. ***a***, Percentage change from baseline (mean ± SEM) for axonal growth and axonal retractions for both *DR6* $^{-/-}$ and WT animals. Solid yellow represents axonal growth *DR6* $^{-/-}$; solid red represents axonal retraction in *DR6* $^{-/-}$ animals; dashed yellow represents axonal growth in WT animals; dashed red represents axonal retraction in the WT animals. ***b***, Temporal dynamics of axonal growth and retraction after whisker plucking. The percentage changes reflect the proportion of added (or subtracted) axons between consecutive imaging time points. ***c***, An example of an axon from a *DR6* $^{-/-}$ mouse 2 d after whisker plucking. There is abnormal morphology of the axon, which projects back toward the cell body. This degree of complex morphology is not observed in WT animals after whisker plucking. We quantified abnormal trajectories of an axonal arbor if the axonal branch at one point deviated >90 degrees from the axis of projection of the axon (see Materials and Methods). Scale bar, 50 μm.

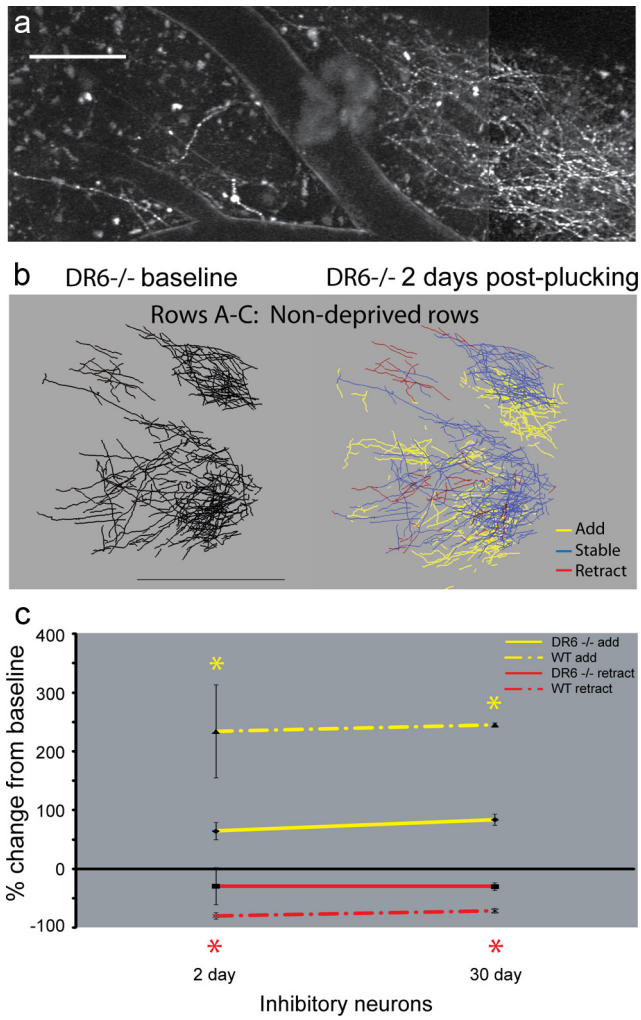

Figure 3. DR6 regulates axonal pruning of inhibitory neurons during periods of experience-dependent plasticity. ***a***, Axons of inhibitory neurons of a *DR6* $^{-/-}$ mouse labeled with GAD65.eGFP.AAV taken with the 2-photon microscope. *Z*-projection of a typical image stack of inhibitory neuron axons. Boutons are visible as bright spots along the axonal length. The large forked structure in the center is a blood vessel, which hides the axons passing underneath. Scale bar, 50 μm. ***b***, Labeled axons of inhibitory neurons whose somata were located in rows D and E (deprived cortex) projecting into nondeprived rows before and 2 d after whisker plucking. Blue represents stable axons that were present during both imaging sessions; red represents axons present during baseline and retracted between the onset of whisker plucking and the second imaging session; yellow represents axons added after the first imaging session and onset of whisker plucking. Scale bar, 400 μm. ***c***, Quantification of axonal dynamics of inhibitory neurons located in LPZ. Percentage change from baseline (mean ± SEM) axonal growth and axonal retractions for both *DR6* $^{-/-}$ and WT animals. Solid yellow represents axonal growth in *DR6* $^{-/-}$ animals; solid red represents axonal retraction in *DR6* $^{-/-}$ animals; dashed yellow represents axonal growth in WT animals; dashed red represents axonal retraction in WT animals.

test). After whisker plucking, there was a small amount of pruning of inhibitory axons in the *DR6* $^{-/-}$ mice, but it was substantially less than that seen in WT animals (Fig. 3*b*, ANOVA, $p = 0.006$). Although the area covered by the inhibitory neuron axons 30 d after plucking increased for *DR6* $^{-/-}$ mice (0.896 ± 0.34 mm^2) relative to WT mice (0.293 ± 0.15 mm^2), the added axonal length was substantially less in the *DR6* mice relative to WT. This may reflect a limit on total axonal "load," where, because of the abnormal baseline extent of inhibitory axons in *DR6* animals, they are limited in their capacity to engage in further outgrowth.

Despite the extensive abnormalities in the axonal response to sensory manipulation, the *DR6* mutant mice are indistinguishable from their WT littermates in terms of manifest behaviors or physical characteristics (e.g., weight, brain size, gait, grooming behavior).

Although the effect of the *DR6* knock-out on axonal pruning was profound, there was little influence on the turnover of boutons on existing axons. Boutons, which are presynaptic axonal specializations, undergo turnover in WT animals even in the absence of altered sensory experience, but whisker plucking produces an increase in the rate of turnover. We compared bouton

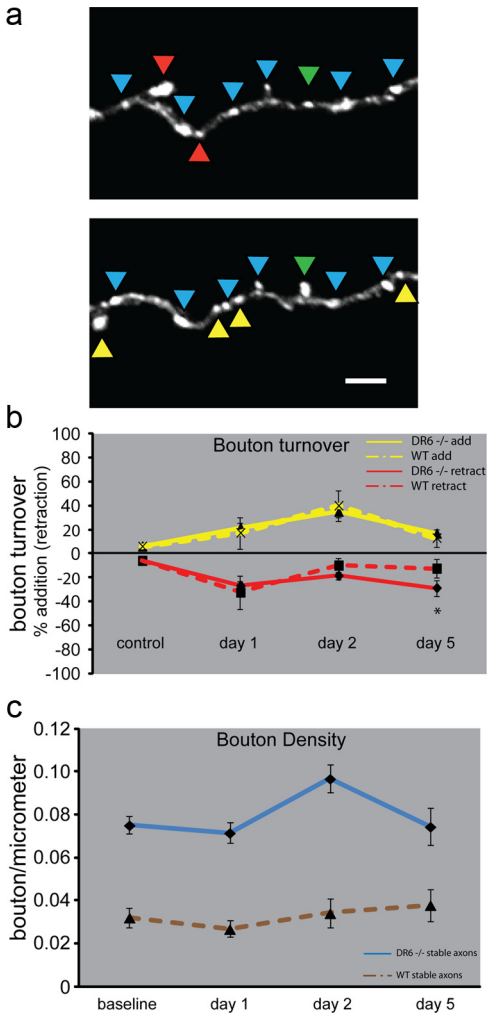

Figure 4. Bouton dynamics in *DR6* knock-out and WT mice. ***a***, A stable axon is shown immediately before whisker plucking (top) and 1 d later (bottom). Blue triangles represent boutons that are stable between the two imaging sessions; green represents boutons that were present at baseline and then became a terminal bouton at day 1; yellow represents boutons added between the imaging sessions; red represents a bouton present at baseline and retracted by day 1. Scale bar, 25 μm. ***b***, Quantification of bouton turnover on stable axons in $DR6^{-/-}$ animals (solid lines) compared with WT littermates (dashed lines; mean ± SEM; $N = 5$ animals). Yellow represents results for boutons that were added; red represents results for boutons that were retracted. Retracted boutons are represented as a negative percentage. ***c***, Bouton density measurements (mean ± SEM; $N = 5$ animals). Blue represents results for boutons located on axons that were stable (i.e., present at all imaging time points) for $DR6^{-/-}$ mice. Brown represents results for boutons located on stable axons for WT littermates.

turnover for stable axons in layer 2/3 in WT and $DR6^{-/-}$ mice over successive time points after whisker plucking, expressed as a percentage of bouton change between consecutive imaging sessions (Fig. 4*b*). Whisker plucking induced a high rate of bouton turnover (both addition and retraction) for both $DR6^{-/-}$ and WT mice (Fig. 4*b*) compared with what was observed in the absence of plucking ($N = 7$). Overall, the rates of bouton addition and removal were similar for the WT and $DR6^{-/-}$ animals ($p < 0.05$ for the early time points), with the exception of a greater rate of retraction at the day 5 time point in the $DR6^{-/-}$ animals ($p = 0.03$). Despite the comparable levels of bouton turnover, the *DR6* mutant animals showed a marked difference in overall bouton density relative to WT animals (Fig. 4*c*), with the $DR6^{-/-}$ showing approximately twice the density of that observed in the WT ($p < 0.0001$). Rather than compensating for the extra axonal arbor by reduced bouton density, the overall synaptic load in the *DR6* mutant animals appears to be greater. But the comparable levels of bouton turnover in $DR6^{-/-}$ animals show that they retain a capacity for circuit modification via synapse elimination, even though they retain axon collaterals that would otherwise be eliminated in the WT.

Discussion

Axonal growth and pruning within the LPZ after manipulating sensory experience is the mechanism by which cortical topography is functionally remapped. Our results indicate that DR6 plays an integral role in the pruning component of axonal plasticity in adult somatosensory cortex. Possibly mirroring the effects of *DR6* knock-out on adult axonal remodeling, the greater extent of axonal arbors observed at baseline in *DR6* mutant mice compared with WT may reflect reduced pruning in the mutant during development. The mutant animals also showed increases in outgrowth into the LPZ compared with WT, which may reflect either the absence of pruning of axons added between imaging sessions or a direct effect of the DR6 pathway on outgrowth in addition to pruning. Our current working hypothesis, based on this and prior studies (Obata et al., 1999; Nikolaev et al., 2009; Simon et al., 2012), is that whisker plucking triggers an increase in BDNF within the deprived cortex, stimulating sprouting but also allowing for DR6 to interact with the amyloid precursor protein and to activate an apoptotic pathway.

In the $DR6^{-/-}$ animals, both excitatory and inhibitory axons had extensive axonal arborizations at baseline that covered a larger territory than the WT animals. Despite the marked differences in the pattern of axonal arborizations in $DR6^{-/-}$ and WT animals, the $DR6^{-/-}$ animals showed no obvious behavioral abnormalities, the topographic map of their whisker barrel system appeared normal, and there was no obvious difference in their brain size. Although one might have expected that the $DR6^{-/-}$ animals could compensate for their inability to prune by removing more synaptic boutons to maintain a constant synaptic load, this did not appear to be the case. To the contrary, $DR6^{-/-}$ excitatory axons had the same rate of bouton turnover and approximately twice the bouton density of WT axons. This suggests that the DR6 pathway may contribute to the regulation of synaptic load by participation in synaptic homeostasis (LeMasson et al., 1993; Turrigiano, 2012) and that this homeostatic mechanism might be disrupted in the $DR6^{-/-}$ animals, a possibility that requires further exploration.

Although it is plausible that, after extended periods of whisker plucking, the cortical circuit could achieve the required pruning in $DR6^{-/-}$ mice by resorting to alternative signal transduction pathways, we did not observe significant pruning, even at the longest time points, for excitatory axons in $DR6^{-/-}$ mice. Even newly sprouted excitatory axons, which tend to be more prone to pruning than the original, stable axons (Yamahachi et al., 2009), showed severely impaired pruning in the $DR6^{-/-}$ animals. Interestingly, however, the axons of inhibitory neurons, although also reduced in the degree of pruning compared with WT animals, did still show pruning. This opens the possibility for the existence of an alternate pathway for pruning that is independent of *DR6*, at least for inhibitory interneurons.

The DR6 pathway has been shown to contribute to axonal pruning occurring during development (Nikolaev et al., 2009). The current study shows that the same mechanisms are recruited during experience-dependent cortical plasticity throughout life. This process mediates the remapping of cortical topography associated with partial removal of cortical inputs, which represents

a functional, rather than a physical, deafferentation, because the thalamic inputs to the cortex remain intact (Darian-Smith and Gilbert, 1995). The changes in adult cortical circuitry have adaptive value for functional recovery after CNS damage or removal of peripheral input (McManus et al., 2008), and they are likely to use mechanisms that are similar to those involved in normal perceptual learning, which also involve changes in lateral cortical interactions (Crist et al., 2001; Li et al., 2004). This raises the intriguing possibility that the DR6 pathway is also involved in the normal experience-dependent changes in cortical function associated with learning.

References

Crist RE, Li W, Gilbert CD (2001) Learning to see: experience and attention in primary visual cortex. Nat Neurosci 4:519–525. CrossRef Medline

Darian-Smith C, Gilbert CD (1994) Axonal sprouting accompanies functional reorganization in adult cat striate cortex. Nature 368:737–740. CrossRef Medline

Darian-Smith C, Gilbert CD (1995) Topographic reorganization in the striate cortex of the adult cat and monkey is cortically mediated. J Neurosci 15:1631–1647. Medline

Fox K (1992) A critical period for experience-dependent synaptic plasticity in rat barrel cortex. J Neurosci 12:1826–1838. Medline

Keck T, Mrsic-Flogel TD, Vaz Afonso M, Eysel UT, Bonhoeffer T, Hübener M (2008) Massive restructuring of neuronal circuits during functional reorganization of adult visual cortex. Nat Neurosci 11:1162–1167. CrossRef Medline

Kossut M, Juliano SL (1999) Anatomical correlates of representational map reorganization induced by partial vibrissectomy in the barrel cortex of adult mice. Neuroscience 92:807–817. CrossRef Medline

LeMasson G, Marder E, Abbott LF (1993) Activity-dependent regulation of conductances in model neurons. Science 259:1915–1917. CrossRef Medline

Li W, Piëch V, Gilbert CD (2004) Perceptual learning and top-down influences in primary visual cortex. Nat Neurosci 7:651–657. CrossRef Medline

Marik SA, Yamahachi H, McManus JN, Szabo G, Gilbert CD (2010) Axonal dynamics of excitatory and inhibitory neurons in somatosensory cortex. PLoS Biol 8:e1000395. CrossRef Medline

McManus JN, Ullman S, Gilbert CD (2008) A computational model of perceptual fill-in following retinal degeneration. J Neurophysiol 99:2086–2100. CrossRef Medline

Nikolaev A, McLaughlin T, O'Leary DD, Tessier-Lavigne M (2009) APP binds DR6 to trigger axon pruning and neuron death via distinct caspases. Nature 457:981–989. CrossRef Medline

Obata S, Obata J, Das A, Gilbert CD (1999) Molecular correlates of topographic reorganization in primary visual cortex following retinal lesions. Cereb Cortex 9:238–248. CrossRef Medline

Portera-Cailliau C, Weimer RM, De Paola V, Caroni P, Svoboda K (2005) Diverse modes of axon elaboration in the developing neocortex. PLoS Biol 3:e272. CrossRef Medline

Simon DJ, Weimer RM, McLaughlin T, Kallop D, Stanger K, Yang J, O'Leary DD, Hannoush RN, Tessier-Lavigne M (2012) A caspase cascade regulating developmental axon degeneration. J Neurosci 32:17540–17553. CrossRef Medline

Turrigiano G (2012) Homeostatic synaptic plasticity: local and global mechanisms for stabilizing neuronal function. Cold Spring Harbor Perspect Biol 4:a005736. CrossRef Medline

Yamahachi H, Marik SA, McManus JN, Denk W, Gilbert CD (2009) Rapid axonal sprouting and pruning accompany functional reorganization in primary visual cortex. Neuron 64:719–729. CrossRef Medline

Zhao H, Yan M, Wang H, Erickson S, Grewal IS, Dixit VM (2001) Impaired c-Jun amino terminal kinase activity and T cell differentiation in death receptor 6-deficient mice. J Exp Med 194:1441–1448. CrossRef Medline